OPEN

The pattern of atrophy in familial Alzheimer disease

Volumetric MRI results from the DIAN study

David M. Cash, PhD*
Gerard R. Ridgway, PhD*
Yuying Liang, MBBS
Natalie S. Ryan, MBBS
Kirsi M. Kinnunen, PhD
Thomas Yeatman, MBBS
Ian B. Malone, PhD
Tammie L.S. Benzinger, MD, PhD
Clifford R. Jack, Jr., MD
Paul M. Thompson, PhD
Bernardino F. Ghetti, MD
Andrew J. Saykin, PsyD
Colin L. Masters, MD
John M. Ringman, MS, MD
Stephen P. Salloway, MD
Peter R. Schofield, PhD, DSc
Reisa A. Sperling, MD
Nigel J. Cairns, PhD
Daniel S. Marcus, PhD
Chengjie Xiong, PhD
Randall J. Bateman, MD
John C. Morris, MD
Martin N. Rossor, MD, FRCP
Sébastien Ourselin, PhD
Nick C. Fox, MD, FRCP
On behalf of the Dominantly Inherited Alzheimer Network (DIAN)

Correspondence to Dr. Ridgway: gerard.ridgway@ucl.ac.uk

Supplemental data at www.neurology.org

ABSTRACT

Objective: To assess regional patterns of gray and white matter atrophy in familial Alzheimer disease (FAD) mutation carriers.

Methods: A total of 192 participants with volumetric T1-weighted MRI, genotyping, and clinical diagnosis were available from the Dominantly Inherited Alzheimer Network. Of these, 69 were presymptomatic mutation carriers, 50 were symptomatic carriers (31 with Clinical Dementia Rating [CDR] = 0.5, 19 with CDR > 0.5), and 73 were noncarriers from the same families. Voxel-based morphometry was used to identify cross-sectional group differences in gray matter and white matter volume.

Results: Significant differences in gray matter ($p < 0.05$, family-wise error–corrected) were observed between noncarriers and mildly symptomatic (CDR = 0.5) carriers in the thalamus and putamen, as well as in the temporal lobe, precuneus, and cingulate gyrus; the same pattern, but with more extensive changes, was seen in those with CDR > 0.5. Significant white matter differences between noncarriers and symptomatic carriers were observed in the cingulum and fornix; these form input and output connections to the medial temporal lobe, cingulate, and precuneus. No differences between noncarriers and presymptomatic carriers survived correction for multiple comparisons, but there was a trend for decreased gray matter in the thalamus for carriers closer to their estimated age at onset. There were no significant increases of gray or white matter in asymptomatic or symptomatic carriers compared to noncarriers.

Conclusions: Atrophy in FAD is observed early, both in areas commonly associated with sporadic Alzheimer disease and also in the putamen and thalamus, 2 regions associated with early amyloid deposition in FAD mutation carriers. *Neurology*® 2013;81:1425–1433

GLOSSARY

AD = Alzheimer disease; **ADNI** = Alzheimer's Disease Neuroimaging Initiative; **aNC** = asymptomatic noncarriers; **CDR** = Clinical Dementia Rating; **DIAN** = Dominantly Inherited Alzheimer Network; **EYO** = estimated years to symptom onset; **FA** = fractional anisotropy; **FAD** = familial Alzheimer disease; **FWE** = family-wise error; **GLM** = general linear model; **GM** = gray matter; **NC** = noncarriers; **PiB** = Pittsburgh compound B; **pMut+** = presymptomatic carriers; **sMut+** = symptomatic carriers; **sNC** = symptomatic noncarriers; **TIV** = total intracranial volume; **VBM** = voxel-based morphometry; **WM** = white matter.

Recent failures of phase III trials[1,2] in Alzheimer disease (AD) have provoked concerns that the mild to moderate dementia stage may be too late for successful treatment.[3,4] Arguably, an effective therapy should be applied at the earliest stages, to slow pathology accumulation and neurodegeneration before substantial irretrievable neuronal loss occurs. Consequently, researchers are designing prevention or secondary prevention studies.[5,6] However, identifying and recruiting at-risk individuals from the general population requires extensive and costly screening,

*These authors contributed equally to this work.

From the Dementia Research Centre (D.M.C., Y.L., N.S.R., K.M.K., T.Y., I.B.M., M.N.R., S.O., N.C.F.) and Wellcome Trust Centre for Neuroimaging (G.R.R.), UCL Institute of Neurology, London, UK; Washington University School of Medicine (T.L.S.B., N.J.C., D.S.M., C.X., R.J.B., J.C.M.), St. Louis, MO; Mayo Clinic (C.R.J.), Rochester, MN; Imaging Genetics Center (P.M.T.), Laboratory of Neuroimaging, Department of Neurology & Psychiatry, UCLA School of Medicine, Los Angeles, CA; Indiana University School of Medicine (B.F.G., A.J.S.), Indianapolis; Mental Health Research Institute (C.L.M.), The University Of Melbourne, Victoria, Australia; Mary S. Easton Center for Alzheimer's Disease (J.M.R.), UCLA Department of Neurology, Los Angeles, CA; Butler Hospital (S.P.S.), Providence, RI; Neuroscience Research Australia (P.R.S.), Sydney; and the Center for Alzheimer Research and Treatment (R.A.S.), Brigham and Women's Hospital, Cambridge, MA.

Coinvestigators are listed on the *Neurology*® Web site at www.neurology.org.

Go to Neurology.org for full disclosures. Funding information and disclosures deemed relevant by the authors, if any, are provided at the end of the article.

with uncertainty that participants will go on to develop AD. Alternatively, individuals carrying an autosomal dominantly inherited mutation for familial AD (FAD) could be targeted. While rare, hundreds of mutation-carrying families have been identified worldwide, with early and relatively predictable ages at onset. Effective therapeutic trials will require sensitive measures of early-stage disease progression, for which imaging shows great promise. Amyloid deposition is evident using PET at least a decade before symptomatic onset in FAD.[7–9] Structural MRI reveals downstream consequences of neurodegeneration that appear closer to symptom onset. At diagnosis of AD dementia, hippocampi are 15% to 20% smaller than in age-matched controls,[10] diverging from normal 3 to 5 years earlier.[11] Some brain regions have produced conflicting results regarding the presence of an early increase in volume.[9,12–17]

Importantly, virtually all previous studies considered a small sample (<25 participants) with a few FAD mutations. We report a voxel-based morphometry study on nearly 200 individuals from the international Dominantly Inherited Alzheimer Network (DIAN),[9] which aims to understand the temporal ordering of abnormalities in FAD.

METHODS

Standard protocol approvals, registrations, and patient consents. All aspects of the study were approved by the institutional review boards for each of the participating sites in DIAN. All participants provided written informed consent.

Participants. All participants were recruited as part of the DIAN study, which aims to enroll up to 400 individuals at risk for one of the genetic mutations linked with FAD. Full details of participating sites, enrollment, and assessments in DIAN have been published.[18] As part of obtaining the family history, a semistructured interview is conducted to determine the affected parent or sibling's age at onset. The estimated years to symptom onset (EYO) has been defined as the difference between this expected age at onset and the participant's current age; negative values indicate that an individual is younger than his or her expected age at onset. Genetic testing is performed to determine the presence of a mutation, but genetic data are provided only to those performing the analysis. This preserves patient confidentiality and ensures that both the participants and the clinicians assessing them remain blind to their genetic status.

At the time of analysis, 242 participants in the DIAN cohort were available from the third data cutoff (February 29, 2012). Of these, 192 had the complete genetic, demographic, and cognitive information required. Participants were divided into 3 groups based on the presence of a mutation and their Clinical Dementia Rating[19] (CDR): 73 were noncarriers (NC); 69 carriers were classified as presymptomatic (pMut+) as their CDR was 0, indicating cognitive normality; and 50 carriers with a CDR of 0.5 or higher were defined as symptomatic (sMut+). Four NC had nonzero CDR, unlikely to be due to coincidental sporadic AD since they were all under 45 years of age, but perhaps arising from non-AD causes such as depression; these therefore formed a fourth group (symptomatic NC [sNC]) separate from the 69 asymptomatic NC (aNC).

MRI scanning. Participants underwent volumetric T1-weighted MRI, using the accelerated sequence defined in the Alzheimer's Disease Neuroimaging Initiative second phase (ADNI-2).[20] Individuals were scanned twice during a session, safeguarding against one poor-quality image. Sites used 3 different types of qualified 3-T scanner: Siemens Tim Trio, Siemens Verio, and Philips Achieva. Matching between scanners and image quality control were performed according to the ADNI protocol by the imaging core.[21]

Image analysis. Voxel-based morphometry (VBM) was carried out using the SPM8 package (Statistical Parametric Mapping; http//www.fil.ion.ucl.ac.uk/spm) running on Matlab 7.12 (MathWorks; http://www.mathworks.com). Gray matter (GM) and white matter (WM) probability maps were obtained from the volumetric images using the tissue segmentation tools in the VBM8 toolbox (University of Jena; http://dbm.neuro.uni-jena.de) to obtain better segmentation of subcortical GM. One individual from the sMut+ group was excluded due to extensive WM pathology. Spatial normalization was performed using DARTEL,[22] modulating normalized tissue maps to preserve their original volumes. Both scans from the imaging session were segmented, but only one from each individual was used in subsequent analysis (chosen as that with the higher SPM segmentation objective function). Images were smoothed using a Gaussian kernel with 6 mm full-width at half-maximum, balancing the detection of small-scale anatomical differences while ameliorating misalignment. GM and WM analysis masks were created by averaging individual smoothed normalized GM and WM segmentations and dichotomizing at a value of 0.2.[23]

Data were fitted with a general linear model (GLM) in SPM8, containing the following terms: a 4-level group factor (aNC, sNC, pMut+, sMut+); a 10-level factor representing the acquisition sites; a 2-level factor indicating the presence of an *APOE* ε4 allele (a well-established risk factor for sporadic AD[24,25]); a factor for gender; a covariate for total intracranial volume (TIV); and a covariate for EYO interacting with the group factor. TIV was calculated by summing GM, WM, and CSF volumes from the VBM8 segmentation. Because multiple participants from the same families enrolled in DIAN, family membership was modeled as a random effect, permitting covariance among relatives. Contrasts of the GLM parameters were used to test for differences among the 3 main diagnostic groups (aNC, pMut+, and sMut+) and among the 10 sites (F contrasts with 2 and 9 numerator degrees of freedom, respectively). Contrasts were also used to detect pairwise differences between diagnostic groups or changes due to *APOE* status (one-tailed t contrasts). Multiple comparison correction was performed to control voxel-level family-wise error (FWE) at $p < 0.05$, though some results are shown at an uncorrected level of $p < 0.001$ (in some cases alongside unthresholded effect maps) to provide better characterization of patterns not reaching significance.

Forthcoming clinical trials may recruit mutation carriers either with mild symptoms or near to their expected onset. Therefore, we performed additional analyses where the carrier groups were divided into smaller subgroups according to criteria relevant for clinical trials. The sMut+ group was divided according to clinical severity as assessed by CDR: 31 individuals with CDR = 0.5 and 19 with CDR > 0.5. The pMut+ group was divided into 3 subgroups

based on EYO: 30 individuals more than 15 years away, 24 between 15 and 6 years away, and 15 less than 6 years from expected onset. As the EYO variable defined these subgroups, the EYO group interaction was replaced with a simple age covariate in this analysis.

RESULTS Demographics of included participants are summarized in table 1. On average, the presymptomatic carriers (pMut+) were more than 10 years away from their expected symptom onset; 80% of carriers have a mutation in the presenilin-1 gene (*PSEN1*), 8% presenilin-2 (*PSEN2*), and 12% amyloid precursor protein (*APP*).

Figure 1 shows the *F* test ($p < 0.05$, FWE corrected) for significant GM differences among the 3 groups of interest: the GM volumes were lower in carriers in 1) the temporal lobe, both medially in the region of the hippocampi and laterally in the temporal neocortex; 2) precuneus; 3) cingulate gyrus, primarily in the posterior region; 4) putamen; and 5) thalamus. For each of these regions, figure 1 provides an illustrative (though circular[26]) plot of the linear fit of GM volume to EYO at the voxel with the peak *F* test statistic. A similar *F* test for WM differences is shown in figure 2. There were significant reductions in the fornix and cingulum, projections to the hippocampus, precuneus, and posterior cingulate. Table e-1 on the *Neurology*® Web site at www.neurology.org details these GM and WM findings. When examining the pairwise comparisons, the *t* test for GM decrease between aNC and sMut+ (figure e-1) looks similar to the overall group test. No findings survived FWE correction when comparing aNC and pMut+.

We performed reverse contrasts to test for GM and WM increases between NC and carriers. For sMut+, there was one area of significantly increased GM on the boundary between the splenium of the corpus callosum and the lateral ventricle. There were 2 findings for WM: the inferior boundary of the caudate and the inferior boundary of the accumbens/putamen. There were no significant increases between aNC and pMut+.

Figure 3 provides GM results when the symptomatic carrier group is subdivided according to CDR. Findings of decreased GM are present even in the mildest symptomatic subgroup (CDR = 0.5). Differences are more widespread in the CDR > 0.5 subgroup despite the smaller sample size. When directly comparing these 2 subgroups, there are significant findings of decreased GM in the more affected (CDR > 0.5) subgroup within the medial temporal lobe and posterior cingulate.

No findings survived FWE correction when comparing EYO-stratified presymptomatic carriers to NC, but there were trends for carriers to show lower GM volume nearer to their expected age at onset. Figure 4 illustrates this trend and provides the effect maps from each EYO subgroup vs NC. In the subgroup less than 5 years away from onset, there is a suggestion of reduced GM in the thalamic areas, and in neocortical areas of the lateral temporal lobe.

DISCUSSION VBM was performed on volumetric MRI from a large cohort of individuals at risk for, or mildly affected by, autosomal dominantly inherited AD from the DIAN study; 192 individuals were studied—a much larger sample than prior FAD studies. The larger sample size in this study can provide a consensus pattern of atrophy, whereas single site studies have provided variable results, likely due to unique patterns of atrophy in the smaller cohorts of mutations and families. We were careful in attempting to account for heterogeneity due to multiple sites and scanners: there were significant effects of site in the peripheral areas of the brain and near the thalamus for

Table 1 Demographics of DIAN participants used in this study

Group	N	% Female	Age, mean (SD)	EYO, mean (SD)	% *PSEN1* mutations
Noncarriers	73	56	40.6 (8.9)	NA	NA
Presymptomatic carriers					
Total	69	58	34.1 (8.9)	−13.1 (8.4)	77
≤−15 EYO	30	53	28.1 (6.7)	−20.7 (4.0)	70
−15 to −6 EYO	24	58	37.1 (5.1)	−11.1 (2.7)	83
≥−5 EYO	15	60	41.3 (9.7)	−1.1 (3.7)	80
Symptomatic carriers					
Total	50	58	45.6 (10.5)	0.1 (8.0)	84
CDR = 0.5	31	61	43.4 (11.0)	−1.5 (8.2)	84
CDR > 0.5	19	53	49.2 (8.6)	2.7 (7.1)	84

Abbreviations: CDR = Clinical Dementia Rating; DIAN = Dominantly Inherited Alzheimer Network; EYO = estimated years to symptom onset; NA = not applicable.

Figure 1 Significant group differences in gray matter volume

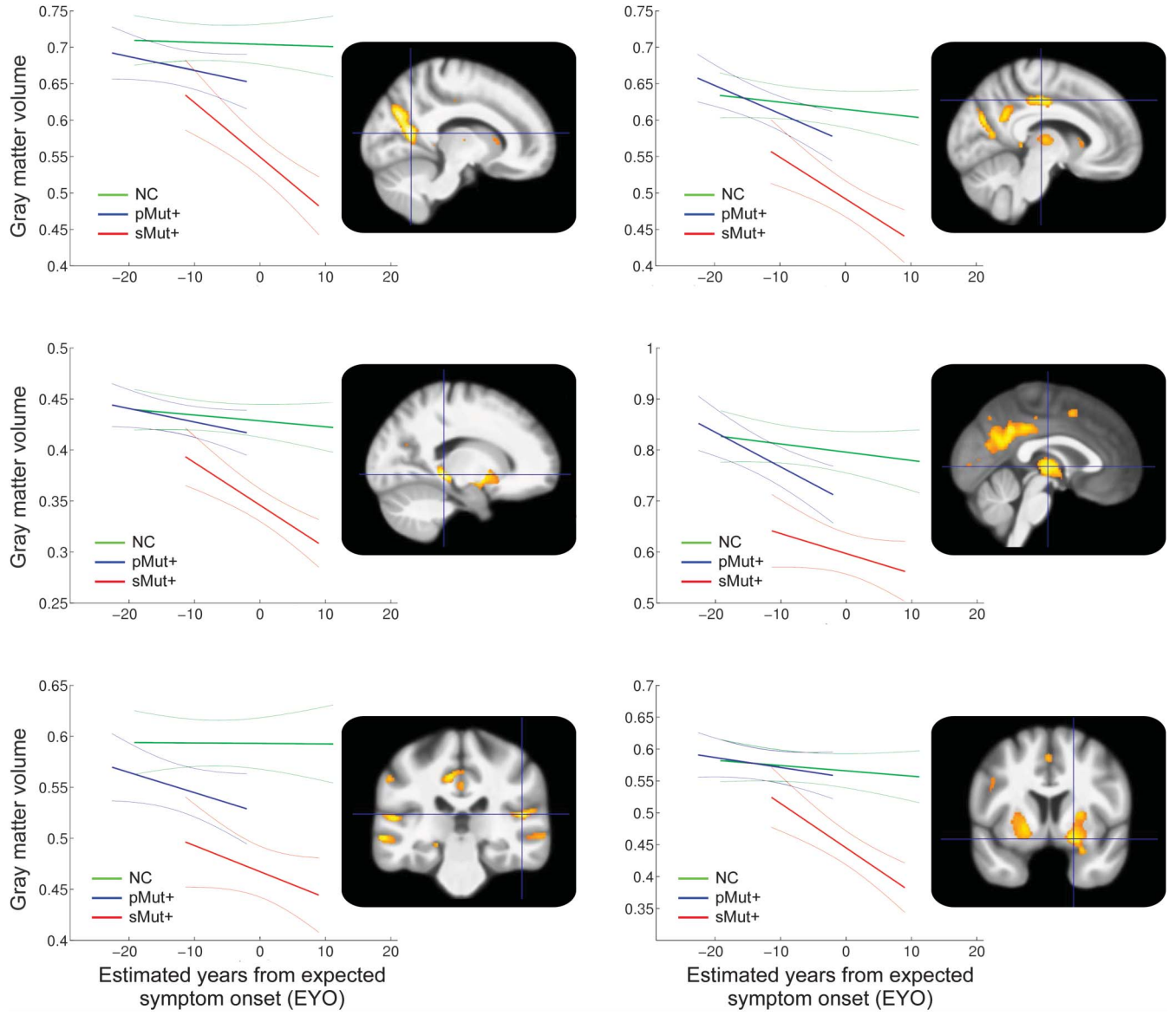

An *F* test was performed among the 3 main groups (asymptomatic noncarriers [NC]; presymptomatic mutation carriers [pMut+]; symptomatic mutation carriers [sMut+]), and all results shown are family-wise error corrected. The peak voxel is highlighted in 6 regions: (left column, top to bottom) precuneus, medial temporal lobe, temporal neocortex; (right column, top to bottom) cingulate, thalamus, putamen. For each voxel highlighted in the 6 slices, a linear fit of the gray matter volume with respect to expected years from symptom onset is plotted. Green lines indicate NC, blue lines indicate pMut+, and red lines indicate sMut+.

GM and in the inferior frontal lobe near the frontal pole for WM (figure e-2), but no significant site-by-group interaction. These findings are mainly in areas frequently affected by differences in hardware and susceptibility artifacts. The site effects show little similarity to the main results, but nevertheless demonstrate the importance of modeling this factor.

We found evidence of GM reduction in 3 areas that are well-recognized in the sporadic (late-onset) AD literature: the temporal lobe, precuneus, and cingulate. There were also signs of early change in the putamen and thalamus—structures not typically associated with sporadic AD, though such an association is documented when comparing patients with AD with elderly subjects who have no objective memory decline.[27,28] In this study, we observed differences in these structures at earlier stages of the disease, with carriers at CDR = 0.5. Recently, decreased volumes and increased fractional anisotropy (FA) of the thalamus and caudate were reported in presymptomatic *PSEN1* mutation carriers[29] (11 participants in that study were also included the current work, though not using the same volumetric T1 scans). These results are interesting in light of amyloid PET studies of FAD that report increased uptake in these areas, which might be the earliest regions of amyloid deposition for some individuals. Striatal uptake of Pittsburgh compound B (PiB) was reported for 5 asymptomatic

Figure 2 Significant group differences in white matter volume

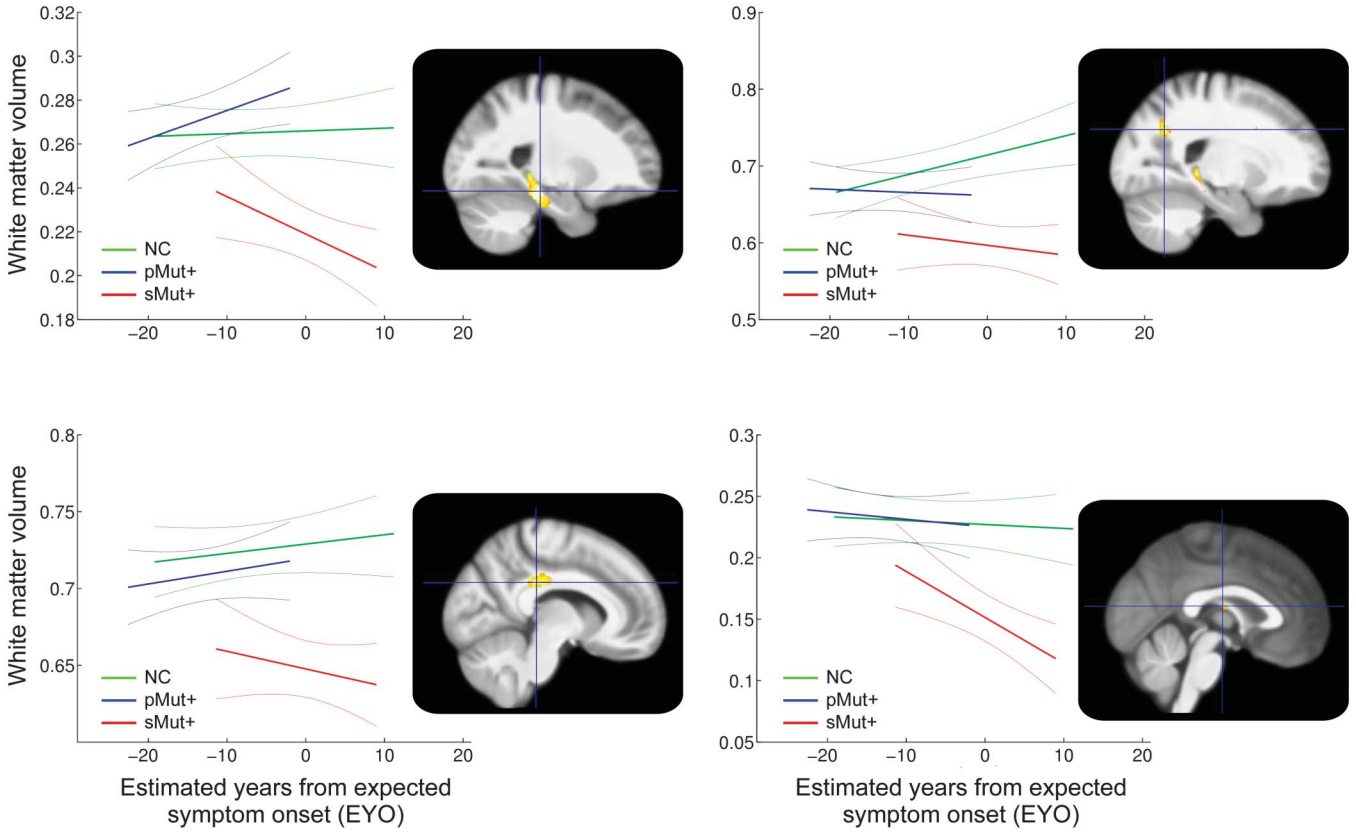

An *F* test was performed among the 3 main groups, and all results shown are family-wise error corrected. The peak voxel is highlighted in 4 regions: (left column, top to bottom) cingulum/perforant path, cingulum (near posterior cingulate); (right column, top to bottom) cingulum (near precuneus), fornix. For each voxel highlighted in the 6 slices, a linear fit of the gray matter volume with respect to expected years from symptom onset is plotted. Green lines indicate asymptomatic noncarriers (NC), blue lines indicate presymptomatic mutation carriers (pMut+), and red lines indicate symptomatic mutation carriers (sMut+).

and 5 symptomatic carriers with 2 *PSEN1* mutations[8]; uptake in cortical areas was also increased compared to controls, though not as much as in sporadic late-onset AD. A similar study of 7 asymptomatic and symptomatic patients with 3 different *PSEN1* mutations found that striatal PiB uptake was not increased compared to sporadic AD, but uptake was increased in the thalamus.[7] However, it remains an open question whether the presence of amyloid alone directly causes atrophy, or whether it is a downstream effect mediated by tau or requiring some other mechanism.[30–32]

WM was reduced in both input (cingulum) and output (fornix) connections to the hippocampi. This is consistent with reported decreases in cross-sectional area and FA of the fornix columns in FAD mutation carriers.[33] We also observed WM differences in areas close to the posterior cingulate and precuneus. However, caution should be exercised when interpreting WM alterations identified using VBM. T1-weighted images provide little anatomical information about WM tracts, so spatial normalization is driven by matching detailed convolutions in GM and the ventricular boundary. Partial volume effects, especially in the small medial temporal structures, could also affect the findings. As most of the WM changes overlap areas that predominantly contain GM, these results may reflect GM atrophy rather than actual WM differences. Future studies using tensor-based morphometry or diffusion-weighted imaging should provide a more complete picture of the WM alterations in FAD.

The majority of the differences observed in this study were in symptomatic mutation carriers. Most of these carriers have a CDR of only 0.5, which usually indicates mild symptoms, insufficient to interfere severely with everyday activities. GM volume reduction was still detectable when the symptomatic carriers with CDR greater than 0.5 were excluded. This suggests that the results were not being driven by the smaller number of more affected individuals, but that changes are already occurring at the time of the first signs of cognitive impairment in FAD. This group is also likely to have a more homogenous pathology than analogous groups in the sporadic AD cohorts.

No significant findings of either increased or decreased GM were present in the presymptomatic carrier group, though a trend toward progressive

Figure 3 Gray matter differences in symptomatic carriers subgrouped by clinical dementia rating

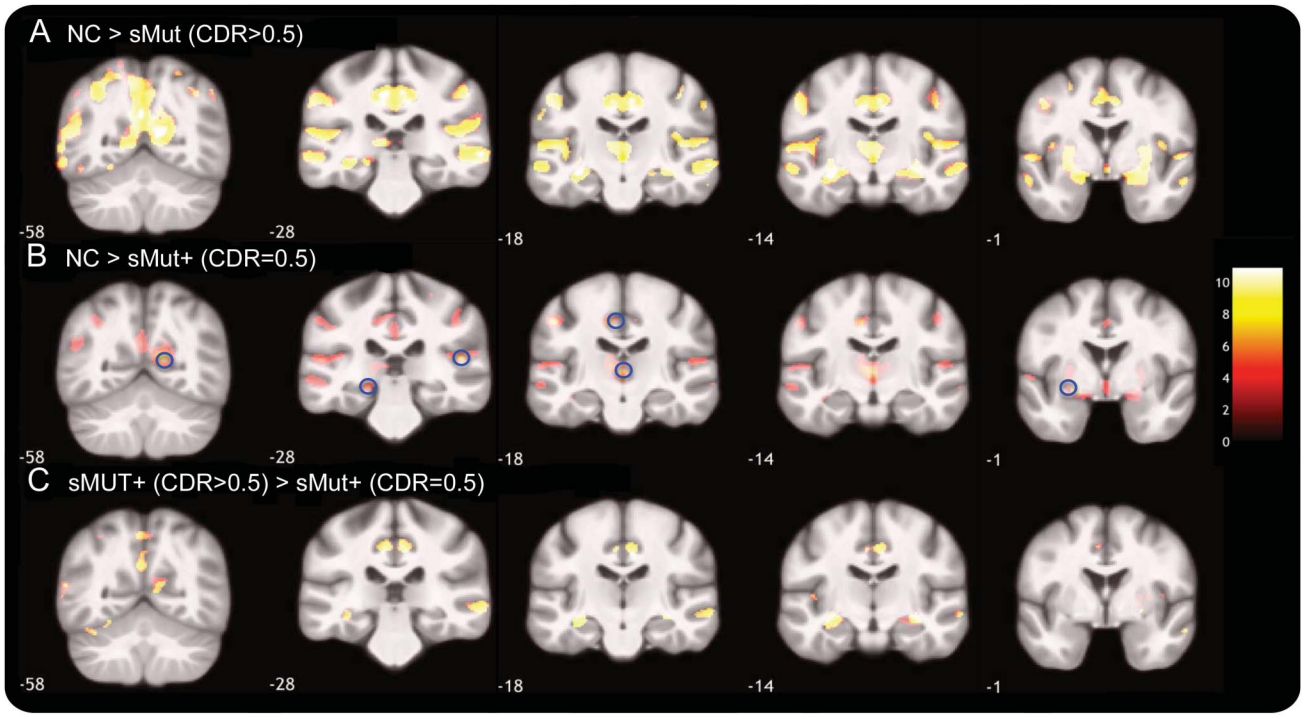

Three pairwise tests are shown: (A) Differences between asymptomatic noncarriers (NC) and symptomatic mutation carriers (sMut+) with Clinical Dementia Rating (CDR) > 0.5 (*t* test, family-wise error [FWE] corrected $p < 0.05$), (B) NC and sMut+ with CDR = 0.5 (*t* test, uncorrected $p < 0.001$), and (C) sMut+ groups, CDR = 0.5 vs CDR > 0.5 (FWE corrected $p < 0.05$). In (B), blue circles indicate the regions where the findings survived FWE correction.

atrophy was suggested by the effect maps of the EYO-based subgroups. Another suggestion of increasing atrophy near to onset is observed when plotting the linear fit of the GM volumes with respect to EYO, shown for key areas in figure 1. Given reports that presymptomatic FAD may feature increased GM volume,[13,14] we also looked at reverse contrasts for areas of increased GM; no findings survived FWE correction. Findings of increased volume may be related to specific mutations and are likely to be subtle in comparison to decreases caused by neurodegeneration, requiring more sensitive measures to identify them. In the symptomatic mutation group, there were some findings of increased volume relative to NC, but given the locations (splenium for GM, caudate and accumbens for WM) and low tissue probabilities, these may reflect partial volume effects.

The earliest point at which GM changes can be observed presymptomatically still needs to be determined. Two structural MRI studies have been performed on the *PSEN1* E280A Colombian kindred to identify changes in presymptomatic carriers compared to age-matched controls. One study[17] using VBM on very young carriers—approximately 20 to 25 years from expected age at onset—found an area of GM decrease in the parietal lobe, which survived correction for multiple comparisons only when using a smaller search volume based on findings for patients with sporadic AD. The other study[15] used carriers much closer (~6 years) to expected onset and observed changes in cortical thickness of the precuneus, angular gyrus, and superior parietal lobule. In a similar sized cohort (25 carriers, 10 NC),[14] there was evidence of GM volume loss in the thalamus and putamen for 9 carriers with CDR of 0, who were on average 15 years before their family's median age at diagnosis. It is not clear how this relates to the time of earliest symptoms, as more than half reported subjective memory complaints.

Our results indicate that widespread GM differences might only occur relatively close to the onset of symptoms. In the at-risk group that we studied, there were only 15 presymptomatic carriers within 5 years of expected age at onset. Having only a small sample in this crucial risk window limits the power to detect changes. VBM is also often less sensitive than targeted volumetric measurements of key structures. Hippocampal volume reductions have been observed as early as 10 years before expected onset in the DIAN cohort.[9] This finding of earlier change could be due to methodologic differences (specifically measuring hippocampal volume as opposed to VBM with correction for multiple comparisons); in addition, the finding may have been partially driven by affected carriers who were younger than their expected age at onset. We plan to use the results from this VBM

Figure 4 Effect maps for subgroups of asymptomatic carriers according to estimated years to symptom onset

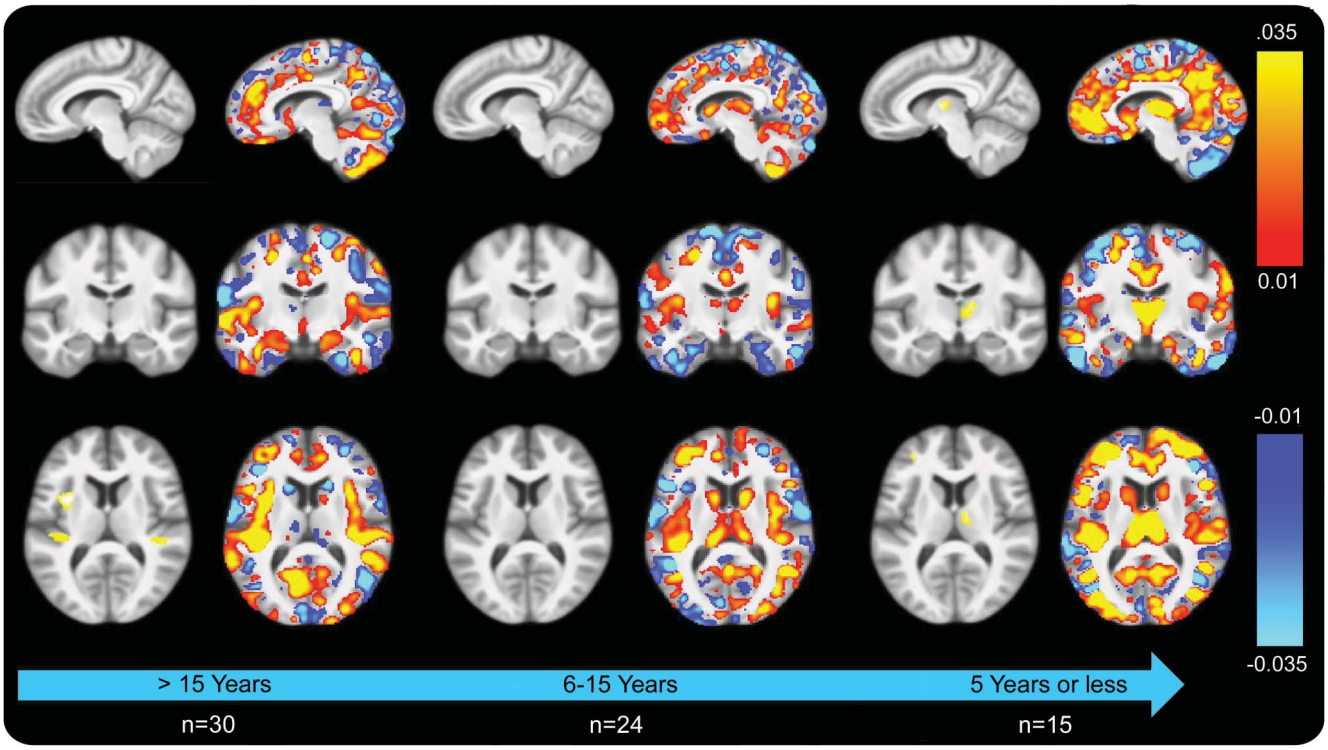

Comparison of noncarriers and asymptomatic carriers with >15 years from onset (left), 6 to 15 years from onset (middle), and less than 5 years from onset (right). For each of the 3 groups, the left column provides findings ($p < 0.001$ uncorrected) and the right column provides the effect maps, with warm colors indicating decreases in gray matter between the asymptomatic subgroup and noncarriers and cool colors indicating increases.

analysis to determine which structures would be of interest for subsequent volumetric analyses.

Furthermore, estimated onset will be inaccurate, due to both true variability in the age at onset over generations and imprecision in determining parental onset. Studies that have information on individuals' actual clinical onsets (i.e., longitudinal studies tracking mutation carriers from presymptomatic to symptomatic stages) are likely to have greater precision in defining the location and timing of losses. Importantly, as part of the DIAN study, the participants studied here will have continued follow-up assessments, including imaging. We expect these longitudinal assessments to enable more sensitive measurement of location, timing, and rate of change in the presymptomatic stages.

In light of previous observations regarding possible clinical,[34] imaging,[35] molecular,[36,37] and neuropathologic differences between individuals with *APP* and *PSEN1* mutations, and among individuals with distinct *PSEN1* mutations,[38] atrophy patterns may differ among these subgroups. Since this study predominantly contains *PSEN1* mutation carriers, it is difficult to determine what differences might be present in FAD caused by *APP*, *PSEN1*, or *PSEN2* mutations. As more participants enroll, it will become clearer whether there are indeed differences in the atrophy patterns among these 3 genes (or even among the more common specific point mutations within these genes). There were no significant findings related to carrying an *APOE* ε4 allele, which could be due to a difference in the roles that the *APOE* gene plays in familial and sporadic AD.

Brain-wide analysis using VBM indicates that individuals with FAD, even when showing the earliest of symptoms, already have significantly less GM in brain areas previously linked to AD, but there also appear to be losses in the putamen and thalamus. This is consistent with prior reports of amyloid deposition in these structures in FAD. These results provide further insight into the pattern of atrophy in FAD, which may help to inform decisions regarding volumetric MRI biomarkers for clinical trials.

AUTHOR CONTRIBUTIONS

Dr. Cash performed the analysis and wrote the manuscript. Dr. Ridgway performed the analysis and wrote the manuscript. Dr. Liang interacted with the patients and collected data at the London DIAN site, as well as assisting with preparation of the manuscript. Dr. Ryan interacted with the patients and collected data at the London DIAN site, as well as assisting with preparation of the manuscript. Dr. Kinnunen assisted in the imaging analysis and preparation of the manuscript. Dr. Yeatmann assisted in the imaging analysis and preparation of the manuscript. Dr. Malone assisted in the imaging analysis and preparation of the manuscript. Dr. Benzinger provided central support as DIAN imaging core leader and assisted in the preparation of the manuscript. Dr. Jack supervised quality checking of all volumetric T1 data and assisted in the preparation of the manuscript. Dr. Thompson was part of the DIAN imaging core and assisted in the preparation of the

manuscript. Dr. Ghetti is the primary investigator at the DIAN IUPUI site and assisted in the preparation of the manuscript. Dr. Saykin is the imaging lead at the DIAN IUPUI site and assisted in the preparation of the manuscript. Dr. Masters is the primary investigator at the DIAN University of Melbourne site and assisted in the preparation of the manuscript. Dr. Ringman is the primary investigator at the DIAN UCLA site and assisted in the preparation of the manuscript. Dr. Salloway is the primary investigator at the DIAN Brown/Butler's site and assisted in the preparation of the manuscript. Dr. Schofield is the primary investigator at the DIAN Neuroscience Research Australia site and assisted in the preparation of the manuscript. Dr. Sperling is the primary investigator at the DIAN Brigham and Women's Hospital site and assisted in the preparation of the manuscript. Dr. Cairns provided central support as the DIAN neuropathology core leader and assisted in the preparation of the manuscript. Dr. Marcus provided central support as the DIAN informatics core leader and assisted in the preparation of the manuscript. Dr. Xiong provided central support as the DIAN biostatistics core leader and assisted in the preparation of the manuscript. Dr. Bateman provided central support as the DIAN clinical core leader and assisted in the preparation of the manuscript. Dr. Morris provided central support as the DIAN chief investigator and assisted in the preparation of the manuscript. Dr. Rossor is the primary investigator at the DIAN UCL site and supervised the design and the preparation of the manuscript. Dr. Ourselin supervised the analysis, the design, and the preparation of the manuscript. Dr. Fox supervised the analysis, the design, and the preparation of the manuscript.

ACKNOWLEDGMENT

This manuscript has been reviewed by DIAN Study investigators for scientific content and consistency of data interpretation with previous DIAN Study publications. They thank the participants and their families and the DIAN research and support staff at each of the participating sites for their contributions to this study (http://www.dian-info.org/personnel.htm).

STUDY FUNDING

Data collection and sharing for this project was supported by The Dominantly Inherited Alzheimer's Network (DIAN, U01AG032438; J.C. Morris, principal investigator) funded by the National Institute on Aging (NIA). Work at UCL was supported by the NIHR Queen Square Dementia BRU. Drs. Cash and Kinnunen are supported by a grant from an anonymous charitable foundation. Drs. Ridgway and Ryan and Professor Fox are supported by the Medical Research Council (grant numbers MR/J014257/1, G0900421, G116/143). Professors Fox and Rossor are NIHR senior investigators. The Dementia Research Centre is an Alzheimer's Research UK Co-ordinating Centre and has also received equipment funded by Alzheimer's Research UK and Brain Research Trust. The Wellcome Trust Centre for Neuroimaging is supported by core funding from the Wellcome Trust (grant number 091593/Z/10/Z).

DISCLOSURE

D. Cash reports no disclosures. G. Ridgway has received honoraria for teaching on SPM courses. Y. Liang, N. Ryan, K. Kinnunen, T. Yeatmann, and I. Malone report no disclosures. T. Benzinger has received personal compensation for activities with Eli Lilly & Company as an advisory board participant and has received research support from Avid Radiopharmaceuticals. C. Jack has received personal compensation for activities with Janssen, Eisai Inc., General Electric, Johnson & Johnson, and Eli Lilly & Company and has received research support from Pfizer Inc., Allon, and Baxter. P. Thompson reports no disclosures. B. Ghetti has received personal compensation for activities with Bayer Pharmaceuticals Corporation and has received research support from the NIA. A. Saykin and C. Masters report no disclosures. J. Ringman has received personal compensation for activities with Takeda Pharmaceuticals and StemCells, Inc. as an advisory board member. Dr. Ringman has received research support from Janssen, Pfizer Inc., Accera, Bristol-Myers Squibb, Inc., and Wyeth Pharmaceuticals. S.P. Salloway reports that he has received support to his hospital for conduct of clinical trials from NIA-ADNI, NIA-DIAN, Alzheimer's Association-DIAN Clinical Trials, Avid Radiopharmaceuticals, Janssen Alzheimer's Immunotherapy, Baxter, BMS, Pfizer, Genentech, GE Healthcare, Roche, Merck, and Biogen. He has served as a consultant for Baxter, Pfizer, Athena, BMS, Merck, Lilly, Roche, GE Healthcare, and Janssen Alzheimer Immunotherapy. P. Schofield reports that his research is supported by NIH (DIAN) and the Wicking Trust for this project. Other grant support comes from the Australian National Health and Medical Research Council, the Australian Research Council, and beyondblue. He has received a speaker fee from Janssen Pharmaceuticals unrelated to this work. R. Sperling has served as a consultant (without personal compensation) for Eli Lilly, Janssen, Avid, and Roche, and as a paid consultant for Merck, Eisai, and Satori. She has received research support from Janssen, Pfizer, Avid, the Alzheimer's Association, American Health Assistance Foundation, Fidelity Biosciences, and the National Institute on Aging. N. Cairns, D. Marcus, and C. Xiong report no disclosures. R. Bateman has received personal compensation for activities with Link Medicine, JAI, Bristol-Myers Squibb Company, Pfizer Inc., Merck, SPRI, Elan Corporation, Eisai Inc., and Medtronic, Inc., received royalty payments from Washington University, and received research support from AstraZeneca Pharmaceuticals and Merck & Co., Inc. He has received personal compensation in an editorial capacity for serving as Associate Editor, *Journal of Neuropsychiatry and Clinical Neurosciences*. J. Morris has participated or is currently participating in clinical trials of antidementia drugs sponsored by the following companies: Janssen Immunotherapy and Pfizer. Dr. Morris has served as a consultant for the following companies: Eisai, Esteve, Janssen Alzheimer Immunotherapy Program, GlaxoSmithKline, Novartis, and Pfizer. He receives research support from Eli Lilly/Avid Radiopharmaceuticals and is funded by NIH grants P50AG005681, P01AG003991, P01AG026276, and U19AG032438. M. Rossor reports no disclosures. S. Ourselin has received personal compensation for activities and research support from IXICO Ltd. He also received financial support for his research from Siemens Molecular Imaging, MIRADA Medical Solution, and General Electric Healthcare. N. Fox reports that his research has received payment for consultancy or for image analysis services from Avid/Lilly, BMS, Elan/Janssen, GE, Lundbeck, and Pfizer/Wyeth. Go to Neurology.org for full disclosures.

Received May 14, 2013. Accepted in final form July 15, 2013.

REFERENCES

1. Green RC, Schneider LS, Amato DA, Beelen AP, Wilcock G. Effect of tarenflurbil on cognitive decline and activities of daily living. JAMA 2009;302:2557–2564.
2. Sampson K. Phase III Alzheimer trial halted: search for therapeutic biomarkers continues. Ann Neurol 2010;68: A9–A12.
3. Golde TE, Schneider LS, Koo EH. Anti-aβ therapeutics in Alzheimer's disease: the need for a paradigm shift. Neuron 2011;69:203–213.
4. Sperling RA, Jack CR Jr, Aisen PS. Testing the right target and right drug at the right stage. Sci Transl Med 2011;3: 111cm33.
5. Bateman RJ, Aisen PS, De Strooper B, Fox NC, Lemere CA, Ringman JM. Autosomal-dominant Alzheimer's disease: a review and proposal for the prevention of Alzheimer's disease. Alzheimers Res Ther 2011;3:1–13.
6. Reiman EM, Langbaum JB, Fleisher AS, et al. Alzheimer's Prevention Initiative: a plan to accelerate the evaluation of presymptomatic treatments. J Alzheimers Dis 2011;26 (suppl 3):321–329.
7. Knight WD, Okello AA, Ryan NS, et al. Carbon-11-Pittsburgh compound B positron emission tomography imaging of amyloid deposition in presenilin 1 mutation carriers. Brain 2011;134:293–300.
8. Klunk WE, Price JC, Mathis CA, et al. Amyloid deposition begins in the striatum of presenilin-1 mutation carriers from two unrelated pedigrees. J Neurosci 2007;27:6174–6184.
9. Bateman RJ, Xiong C, Benzinger TL, et al. Clinical and biomarker changes in dominantly inherited Alzheimer's disease. N Engl J Med 2012;367:795–804.
10. Fox NC, Warrington EK, Freeborough PA, Hartikainen P, Kennedy AM. Presymptomatic hippocampal atrophy in

Alzheimer's disease: a longitudinal MRI study. Brain 1996; 119:2001–2007.
11. Schott JM, Fox NC, Frost C, et al. Assessing the onset of structural change in familial Alzheimer's disease. Ann Neurol 2003;53:181–188.
12. Knight WD, Kim LG, Douiri A, Frost C, Rossor MN, Fox NC. Acceleration of cortical thinning in familial Alzheimer's disease. Neurobiol Aging 2011;32:1765–1773.
13. Fortea J, Sala-Llonch R, Bartrés-Faz D, et al. Increased cortical thickness and caudate volume precede atrophy in PSEN1 mutation carriers. J Alzheimers Dis 2010;22: 909–922.
14. Lee GJ, Lu PH, Medina LD, et al. Regional brain volume differences in symptomatic and presymptomatic carriers of familial Alzheimer's disease mutations. J Neurol Neurosurg Psychiatry 2013;84:154–162.
15. Quiroz YT, Stern CE, Reiman EM, et al. Cortical atrophy in presymptomatic Alzheimer's disease presenilin 1 mutation carriers. J Neurol Neurosurg Psychiatry 2013;84: 556–561.
16. Apostolova LG, Hwang KS, Medina LD, et al. Cortical and hippocampal atrophy in patients with autosomal dominant familial Alzheimer's disease. Dement Geriatr Cogn Disord 2011;32:118–125.
17. Reiman EM, Quiroz YT, Fleisher AS, et al. Brain imaging and fluid biomarker analysis in young adults at genetic risk for autosomal dominant Alzheimer's disease in the presenilin 1 E280A kindred: a case-control study. Lancet Neurol 2012;11:1048–1056.
18. Morris JC, Aisen PS, Bateman RJ, et al. Developing an international network for Alzheimer research: the dominantly inherited Alzheimer network. Clin Invest 2012;2: 975–984.
19. Morris JC. The Clinical Dementia Rating (CDR): current version and scoring rules. Neurology 1993;43:2412–2414.
20. Jack CR, Bernstein MA, Borowski BJ, et al. Update on the magnetic resonance imaging core of the Alzheimer's Disease Neuroimaging Initiative. Alzheimers Dement 2010;6: 212–220.
21. Jack CR, Bernstein MA, Fox NC, et al. The Alzheimer's Disease Neuroimaging Initiative (ADNI): MRI methods. J Magn Reson Imaging 2008;27:685–691.
22. Ashburner J. A fast diffeomorphic image registration algorithm. Neuroimage 2007;38:95–113.
23. Ridgway GR, Omar R, Ourselin S, Hill DLG, Warren JD, Fox NC. Issues with threshold masking in voxel-based morphometry of atrophied brains. Neuroimage 2009;44: 99–111.
24. Gutiérrez-Galve L, Lehmann M, Hobbs NZ, et al. Patterns of cortical thickness according to APOE genotype in Alzheimer's disease. Dement Geriatr Cogn Disord 2009; 28:476–485.
25. Jagust W. Apolipoprotein E, neurodegeneration, and Alzheimer disease. Arch Neurol 2012;70:1–2.
26. Kriegeskorte N, Lindquist MA, Nichols TE, Poldrack RA, Vul E. Everything you never wanted to know about circular analysis, but were afraid to ask. J Cereb Blood Flow Metab 2010;30:1551–1557.
27. De Jong LW, Van der Hiele K, Veer IM, et al. Strongly reduced volumes of putamen and thalamus in Alzheimer's disease: an MRI study. Brain 2008;131:3277–3285.
28. Fjell AM, Walhovd KB, Fennema-Notestine C, et al. One-year brain atrophy evident in healthy aging. J Neurosci 2009;29:15223–15231.
29. Ryan NS, Keihaninejad S, Shakespeare TJ, et al. MRI evidence for presymptomatic change in thalamus and caudate in familial Alzheimer's disease. Brain 2013;136: 1399–1414.
30. Wirth M, Madison CM, Rabinovici GD, Oh H, Landau SM, Jagust WJ. Alzheimer's disease neurodegenerative biomarkers are associated with decreased cognitive function but not -amyloid in cognitively normal older individuals. J Neurosci 2013;33:5553–5563.
31. Desikan RS, McEvoy LK, Thompson WK, et al. Amyloid-β-associated clinical decline occurs only in the presence of elevated p-tau. Arch Neurol 2012;69:709–713.
32. Fjell AM, Walhovd KB. Neuroimaging results impose new views on Alzheimer's disease: the role of amyloid revised. Mol Neurobiol 2012;45:153–172.
33. Ringman JM, O'Neill J, Geschwind D, et al. Diffusion tensor imaging in preclinical and presymptomatic carriers of familial Alzheimer's disease mutations. Brain 2007;130: 1767–1776.
34. Ryan NS, Rossor MN. Correlating familial Alzheimer's disease gene mutations with clinical phenotype. Biomark Med 2010;4:99–112.
35. Scahill RI, Ridgway GR, Bartlett JW, et al. Genetic influences on atrophy patterns in familial Alzheimer's disease: a comparison of APP and PSEN1 mutations. J Alzheimers Dis 2013;35:199–212.
36. Chávez-Gutiérrez L, Bammens L, Benilova I, et al. The mechanism of γ-secretase dysfunction in familial Alzheimer disease. EMBO J 2012;31:2261–2274.
37. Gessel MM, Bernstein S, Kemper M, Teplow DB, Bowers MT. Familial Alzheimer's disease mutations differentially alter amyloid β-protein oligomerization. ACS Chem Neurosci 2012;3:909–918.
38. Shepherd C, McCann H, Halliday GM. Variations in the neuropathology of familial Alzheimer's disease. Acta Neuropathol 2009;118:37–52.